Journal of Sound and Vibration (1997) **199**(4), 595–613

FREE VIBRATION OF SHEAR-DEFORMABLE GENERAL TRIANGULAR PLATES

W. KARUNASENA

Department of Civil and Systems Engineering, James Cook University of North Queensland Townsville, Queensland 4811 *Australia*

AND

S. KITIPORNCHAI

Department of Civil Engineering, The University of Queensland, Brisbane, Queensland 4072, *Australia*

(*Received* 18 *September* 1995, *and in final form* 22 *April* 1996)

An analysis of free vibration of shear-deformable general triangular plates with arbitrary combinations of boundary conditions is presented. The Reissner-Mindlin plate theory is used to incorporate shear deformation effects in the analysis. The triangular plate is first mapped onto a basic square plate. The Rayleigh–Ritz method with an admissible displacement function expressed as a product of a two-dimensional simple polynomial and a basic function is then used to obtain the governing eigenvalue equation. The basic function is chosen as the product of boundary expressions of the basic square plate, each raised to an appropriate power to satisfy the various geometric boundary conditions of the actual triangular plate. Gaussian quadrature is used for numerical evaluation of stiffness and mass matrices. The natural frequencies of general triangular Mindlin plates with different combinations of free, simply supported and clamped conditions are determined. Wherever possible, the results are verified by comparison with existing published solutions. A comprehensive parametric study of natural frequencies of general triangular plates with all three edges clamped is presented graphically. No previous results are known to exist for general triangular Mindlin plates having arbitrary combinations of boundary conditions.

1. INTRODUCTION

The free vibration of thin triangular plates has been thoroughly investigated by many researchers, and most of the early developments have been well documented by Leissa [1–4]. Recently, the Rayleigh–Ritz method with two-dimensional polynomial functions as the admissible functions has been used by several researchers [5–9] to analyse the vibration of thin triangular plates.

The classical thin plate theory cannot be used for thick plates, since it does not take into account the effect for deformation due to transverse shear. This results in over-estimation of vibration frequencies. To allow for this effect, Reissner [10] and Mindlin [11] have proposed a first order theory that assumes a constant transverse shear-strain distribution through the plate thickness. A shear correction factor κ is then introduced to compensate for the errors resulting from the approximation of the non-uniform shear-strain distribution.

Only a limited number of studies concerning free vibration of thick triangular plates have been reported in the literature. McGee *et al*. [12] used a finite element analysis that

0022–460X/97/040595 + 19 $25.00/0/sv960613

incorporates a higher order shear deformation theory to compute the natural frequencies of cantilevered skewed thick plates. Due to the higher order shear deformation theory, the finite element analysis involved nine-degrees-of-freedom per node. Recently, Kitipornchai *et al*. [13] investigated the free vibration of isosceles triangular thick plates with arbitrary combinations of boundary conditions along the edges, using a Rayleigh–Ritz approach in conjunction with the first order Mindlin shear deformation theory.

However, the more general problem of free vibration of general triangular thick plates with arbitrary combinations of free, simply supported and clamped boundary conditions has not received attention in the past. The aim of this paper is to provide a numerical solution to this problem based on Mindlin shear deformation theory. The analysis uses the pb-2 Rayleigh–Ritz method [13–16] which has been shown to be simple and efficient. The actual triangular plate is first mapped onto a basic square domain as shown in Figure 1. The Ritz functions are defined over the basic square domain by the product of a two-dimensional polynomial (p-2) and a basic function (b). The basic function is then formed from the product of equations of the mapped boundaries, each raised to an appropriate power, to satisfy various geometric boundary conditions. Gaussian quadrature is used to integrate numerically the stiffness and mass matrices over the domain of the basic square plate.

To illustrate the validity of the solutions, convergence tests have been carried out and comparisons have been made with existing published values from the open literature. The natural frequencies of general triangular Mindlin plates with different combinations of free, simply supported and clamped conditions are tabulated. A comprehensive parametric study of natural frequencies of general triangular plates with all three edges clamped is presented graphically.

2. MATHEMATICAL FORMULATION

Consider a flat, isotropic, thick, general triangular shaped plate of uniform thickness t, Young's modulus E, shear modulus G, and Poisson's ratio v. The Cartesian co-ordinate system x-y and the geometry of the plate with two adjoining side lengths a, b and internal angle α between these two sides are as defined in Figure 1(a). The plate may have prescribed combination of support edge conditions. The problem is to determine the free vibration frequencies of the plate.

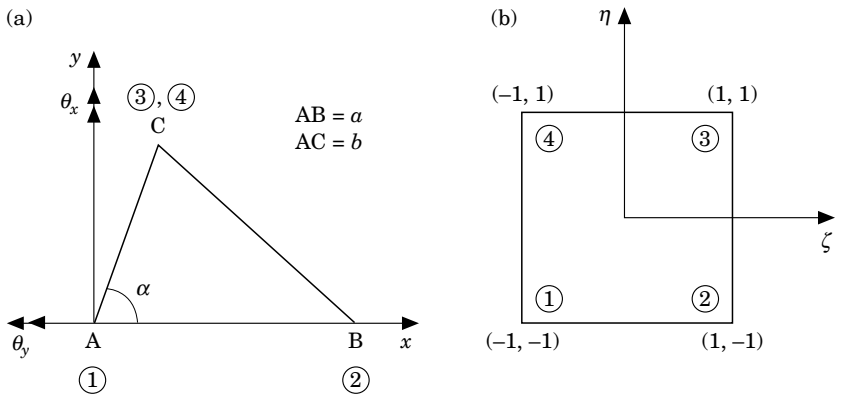

Figure 1. Geometry and co-ordinate systems: (a) Actual triangular plate in the x-y co-ordinate system; (b) mapped plate in the ζ-η co-ordinate system.

2.1. ENERGY FUNCTIONAL

Using Mindlin's shear deformation theory, the energy functional Π can be written in terms of the maximum strain energy U_{max} and the maximum kinetic energy $T_{\max}$ as (see [13])

$$\Pi = U_{max} - T_{max} \tag{1}$$

where

$$U_{max} = \frac{1}{2}\int_A \left(D\left\{\left(\frac{\partial\theta_x}{\partial x} + \frac{\partial\theta_y}{\partial y}\right)^2 - 2(1-\nu)\left[\frac{\partial\theta_x}{\partial x}\frac{\partial\theta_y}{\partial y} - \frac{1}{4}\left(\frac{\partial\theta_x}{\partial x} + \frac{\partial\theta_y}{\partial x}\right)^2\right]\right\}\right.$$

$$\left. + \kappa G t[(\theta_x + \partial w/\partial x)^2 + (\theta_y + \partial w/\partial y)^2]\right) \mathrm{d}A, \tag{2}$$

$$T_{max} = \tfrac{1}{2}\Omega^2 \int_A [\rho t w^2 + \tfrac{1}{12}\rho t^3(\theta_x^2 + \theta_y^2)]\, \mathrm{d}A, \tag{3}$$

in which A = area of the plate; w = transverse deflection; θ_x = rotation about the y-axis; θ_y = rotation about the x-axis; Ω = angular frequency; ρ = plate density per unit volume; D = flexural rigidity of plate = $Et^3/[12(1-\nu^2]$. For convenience in numerical integration, the actual triangular plate in the x-y plane is mapped onto a 2×2 basic square plate in the ζ-η plane (as shown in Figure 1(b)) using the co-ordinate transformation given by

$$x = \tfrac{1}{4}(1+\zeta)(1-\eta)a + \tfrac{1}{2}(1+\eta)b\cos\alpha, \qquad y = \tfrac{1}{2}(1+\eta)b\sin\alpha. \tag{4a–4b}$$

Applying the chain rule of differentiation, the first derivative of any quantity () in the two co-ordinate systems can be related by

$$\begin{Bmatrix} \partial()/\partial x \\ \partial()/\partial y \end{Bmatrix} = \mathbf{J}^{-1} \begin{Bmatrix} \partial()/\partial\zeta \\ \partial()/\partial\eta \end{Bmatrix}, \tag{5}$$

where $\mathbf{J}$ is the Jacobian matrix of the co-ordinate transformation given by

$$\mathbf{J} = \begin{bmatrix} \partial x/\partial\zeta & \partial y/\partial\zeta \\ \partial x/\partial\eta & \partial y/\partial\eta \end{bmatrix}. \tag{6}$$

Equations (5) and (6) will be used later to transform the x-y domain integrals of the energy functional into ζ-η domain integrals.

2.2. RITZ FUNCTIONS

For Mindlin plates, the transverse deflection and rotations may be parameterized by a set of Ritz functions chosen as two-dimensional polynomials in the ζ-η plane as

$$w(\zeta,\eta) = \sum_{r=0}^{p_1}\sum_{s=0}^{r} c_i\phi_i(\zeta,\eta) = \sum_{i=1}^{m} c_i\phi_i(\zeta,\eta) = \mathbf{c}^{\mathrm{T}}\boldsymbol{\phi}, \tag{7a}$$

$$\theta_x(\zeta,\eta) = \sum_{r=0}^{p_2}\sum_{s=0}^{r} d_i\psi_{xi}(\zeta,\eta) = \sum_{i=1}^{n} d_i\psi_{xi}(\zeta,\eta) = \mathbf{d}^{\mathrm{T}}\boldsymbol{\psi}_{\mathbf{x}}, \tag{7b}$$

$$\theta(\zeta,\eta) = \sum_{r=0}^{p_3}\sum_{s=0}^{r} e_i\psi_{yi}(\zeta,\eta) = \sum_{i=1}^{l} e_i\psi_{yi}(\zeta,\eta) = \mathbf{e}^{\mathrm{T}}\boldsymbol{\psi}_{\mathbf{y}}, \tag{7c}$$

where $p_s (s = 1, 2, 3)$ is the degree of the mathematically complete two-dimensional polynomial space; c_i, d_i, and e_i are the known coefficients to be varied with the subscript i given by

$$i = (r + 1)(r + 2)/2 - (r - s); \tag{8}$$

c, **d**, **e** are the unknown coefficient vectors having c_i, d_i, e_i as respective elements; m, n, l are, respectively, the dimensions of **c**, **d**, **e** given by

$$m = \tfrac{1}{2}(p_1 + 1)(p_1 + 2), \qquad n = \tfrac{1}{2}(p_2 + 1)(p_2 + 2), \qquad l = \tfrac{1}{2}(p_3 + 1)(p_3 + 2); \tag{9a–c}$$

and $\boldsymbol{\phi}$, $\boldsymbol{\psi}_x$, $\boldsymbol{\psi}_y$ are the pb-2 Ritz function vectors whose ith elements are given by

$$\phi_i = f_i \phi_1, \qquad \psi_{xi} = f_i \psi_{x1}, \qquad \psi_{yi} = f_i \psi_{y1}, \tag{10a–c}$$

where

$$f_i = \zeta^{r-s} \eta^s. \tag{11}$$

Here, ϕ_1, ψ_{x1}, and ψ_{y1} are the basic functions which are chosen as products of the boundary expression functions to ensure the automatic satisfaction of geometric boundary conditions.

As explained in detail in [13], four types of edge conditions can be identified for Mindlin type plates. These are free edge (F), clamped edge (C), the first kind of simply supported edge (S), and the second kind of simply supported edge (S*). The S condition requires the transverse deflection and tangential rotation along the supported edge to be zero while the S* condition requires only the transverse deflection along the support to be zero. The basic functions are chosen as products of the boundary expressions to ensure the automatic satisfaction of geometric boundary conditions. These functions are given by

$$\phi_1 = (\eta + 1)^{\Theta_1} (\zeta - 1)^{\Theta_2} (\zeta + 1)^{\Theta_3}, \qquad \psi_{x1} = (\eta + 1)^{\Theta_4} (\zeta - 1)^{\Theta_5} (\zeta + 1)^{\Theta_6},$$
$$\psi_{y1} = (\eta + 1)^{\Theta_7} (\zeta - 1)^{\Theta_8} (\zeta + 1)^{\Theta_9}, \tag{12a–c}$$

where $\Theta_j, j = 1, 2, \ldots, 9$ takes different values (0 or 1) according to different boundary conditions as follows:

1. For side AB, if the edge is free (F): $\Theta_1 = \Theta_4 = \Theta_7 = 0$. (13a)
   If the edge is clamped (C): $\Theta_1 = \Theta_4 = \Theta_7 = 1$. (13b)
   If the edge is simply supported (S): $\Theta_1 = \Theta_4 = 1, \quad \Theta_7 = 0$. (13c)
   If the edge is simply supported (S*): $\Theta_1 = 1, \quad \Theta_4 = \Theta_7 = 0$. (13d)

2. For side BC, if the edge is free (F): $\Theta_2 = \Theta_5 = \Theta_8 = 0$. (14a)
   If the edge is clamped (C): $\Theta_2 = \Theta_5 = \Theta_8 = 1$. (14b)
   If the edge is simply supported (S*): $\Theta_2 = 1, \quad \Theta_5 = \Theta_8 = 0$. (14c)

3. For side CA, if the edge is free (F): $\Theta_3 = \Theta_6 = \Theta_9 = 0$. (15a)
   If the edge is clamped (C): $\Theta_3 = \Theta_6 = \Theta_9 = 1$. (15b)
   If the edge is simply supported (S*): $\Theta_3 = 1, \quad \Theta_6 = \Theta_9 = 0$. (15c)

The Ritz functions constructed using the above defined basic functions can satisfy the geometric boundary conditions for all but one special case. The exception is for the S edge condition where the S edge is inclined to the Cartesian x-y axes. Therefore, this analysis applies to Mindlin plates with any combinations of C, F, S* and S edge conditions. However, at most only one S edge can be included in the analysis of general triangular shaped plates by choosing the x-axis along the S edge. For the special case of delta

(right-angled) triangular plates, two S edges can be treated in the analysis by orienting the x-y axes to make them parallel to the two edges that make the right angle.

2.3. GOVERNING EIGENVALUE PROBLEM

Applying the Rayleigh–Ritz method,

$$\frac{\partial \Pi}{\partial c_i} = 0, \quad i = 1, 2, \ldots, m, \qquad \frac{\partial \Pi}{\partial d_i} = 0, \quad i = 1, 2, \ldots, n, \qquad \frac{\partial \Pi}{\partial e_i} = 0, \quad i = 1, 2, \ldots, l. \tag{16a–c}$$

Transforming the integration domain of the integrals in equations (2) and (3) into the ζ-η plane and substituting equations (1–15) into (16) results in

$$(\mathbf{K} - \Omega^2 \mathbf{M})\mathbf{q} = \mathbf{0}, \tag{17}$$

where

$$\mathbf{q}^{\mathrm{T}} = \langle \mathbf{c}^{\mathrm{T}} \quad \mathbf{d}^{\mathrm{T}} \quad \mathbf{e}^{\mathrm{T}} \rangle, \qquad \mathbf{K} = \begin{bmatrix} \mathbf{K}_{\mathbf{cc}} & \mathbf{K}_{\mathbf{cd}} & \mathbf{K}_{\mathbf{ce}} \\ & \mathbf{K}_{\mathbf{dd}} & \mathbf{K}_{\mathbf{de}} \\ \text{symmetric} & & \mathbf{K}_{\mathbf{ee}} \end{bmatrix}, \qquad \mathbf{M} = \begin{bmatrix} \mathbf{M}_{\mathbf{cc}} & \mathbf{M}_{\mathbf{cd}} & \mathbf{M}_{\mathbf{ce}} \\ & \mathbf{M}_{\mathbf{dd}} & \mathbf{M}_{\mathbf{de}} \\ \text{symmetric} & & \mathbf{M}_{\mathbf{ee}} \end{bmatrix} \tag{18–20}$$

and the submatrices inside $\mathbf{K}$ and $\mathbf{M}$ are given by

$$\mathbf{K}_{\mathbf{cc}} = \kappa G t \int_{\bar{A}} \left(\frac{\partial \boldsymbol{\phi}}{\partial x} \frac{\partial \boldsymbol{\phi}^{\mathrm{T}}}{\partial x} + \frac{\partial \boldsymbol{\phi}}{\partial y} \frac{\partial \boldsymbol{\phi}^{\mathrm{T}}}{\partial y} \right) |\mathbf{J}| \, \mathrm{d}\bar{A}, \tag{21a}$$

$$\mathbf{K}_{\mathbf{cd}} = \kappa G t \int_{\bar{A}} \frac{\partial \boldsymbol{\phi}}{\partial x} \boldsymbol{\psi}_x^{\mathrm{T}} |\mathbf{J}| \, \mathrm{d}\bar{A}, \qquad \mathbf{K}_{\mathbf{ce}} = \kappa G t \int_{\bar{A}} \frac{\partial \boldsymbol{\phi}}{\partial y} \boldsymbol{\psi}_y^{\mathrm{T}} |\mathbf{J}| \, \mathrm{d}\bar{A}, \tag{21b, c}$$

$$\mathbf{K}_{\mathbf{dd}} = D \int_{\bar{A}} \left(\frac{\partial \boldsymbol{\psi}_x}{\partial x} \frac{\partial \boldsymbol{\psi}_x^{\mathrm{T}}}{\partial x} + \left(\frac{1 - \nu}{2} \right) \frac{\partial \boldsymbol{\psi}_x}{\partial y} \frac{\partial \boldsymbol{\psi}_x^{\mathrm{T}}}{\partial y} + \frac{\kappa G t}{D} \boldsymbol{\psi}_x \boldsymbol{\psi}_x^{\mathrm{T}} \right) |\mathbf{J}| \, \mathrm{d}\bar{A}, \tag{21d}$$

$$\mathbf{K}_{\mathbf{de}} = D \int_{\bar{A}} \left(\nu \frac{\partial \boldsymbol{\psi}_x}{\partial x} \frac{\partial \boldsymbol{\psi}_y^{\mathrm{T}}}{\partial y} + \left(\frac{1 - \nu}{2} \right) \frac{\partial \boldsymbol{\psi}_x}{\partial y} \frac{\partial \boldsymbol{\psi}_y^{\mathrm{T}}}{\partial x} \right) |\mathbf{J}| \, \mathrm{d}\bar{A}, \tag{21e}$$

$$\mathbf{K}_{\mathbf{ee}} = D \int_{\bar{A}} \left(\frac{\partial \boldsymbol{\psi}_y}{\partial y} \frac{\partial \boldsymbol{\psi}_y^{\mathrm{T}}}{\partial y} + \left(\frac{1 - \nu}{2} \right) \frac{\partial \boldsymbol{\psi}_y}{\partial x} \frac{\partial \boldsymbol{\psi}_y^{\mathrm{T}}}{\partial x} + \frac{\kappa G t}{D} \boldsymbol{\psi}_y \boldsymbol{\psi}_y^{\mathrm{T}} \right) |\mathbf{J}| \, \mathrm{d}\bar{A}. \tag{21f}$$

$$\mathbf{M}_{\mathbf{cc}} = \rho t \int_{\bar{A}} \boldsymbol{\phi} \boldsymbol{\phi}^{\mathrm{T}} |\mathbf{J}| \, \mathrm{d}\bar{A}, \qquad \mathbf{M}_{\mathbf{cd}} = \mathbf{0}, \qquad \mathbf{M}_{\mathbf{ce}} = \mathbf{0}, \tag{22a–c}$$

$$\mathbf{M}_{\mathbf{dd}} = \tfrac{1}{12} \rho t^3 \int_{\bar{A}} \boldsymbol{\psi}_x \boldsymbol{\psi}_x^{\mathrm{T}} |\mathbf{J}| \, \mathrm{d}\bar{A}, \qquad \mathbf{M}_{\mathbf{de}} = \mathbf{0}, \qquad \mathbf{M}_{\mathbf{ee}} = \tfrac{1}{12} \rho t^3 \int_{\bar{A}} \boldsymbol{\psi}_y \boldsymbol{\psi}_y^{\mathrm{T}} |\mathbf{J}| \, \mathrm{d}\bar{A}, \tag{22d–f}$$

in which $\mathbf{K}$ and $\mathbf{M}$ represent the stiffness and mass matrices of the plate respectively, and $\bar{A}$ denotes the area of the basic square plate. The free vibration characteristics of the triangular Mindlin plate are governed by the first order eigenvalue problem in equation

TABLE 1

Convergence of frequency parameters λ for SCF plates when $b/a = 2{\cdot}0$

			Mode sequence number					
$\alpha(^\circ)$	t/a	$p_1 = p_2 = p_3$	1	2	3	4	5	6
45	0·001	6	1·411	3·546	7·631	9·845	15·887	23·017
		8	1·385	3·339	5·564	7·909	9·928	13·826
		10	1·382	3·303	5·310	7·410	8·595	12·005
		12	1·382	3·301	5·292	7·301	8·315	11·088
		13	1·381	3·301	5·291	7·292	8·295	11·026
		14	1·381	3·301	5·290	7·290	8·289	10·941
	0·1	6	1·331	3·098	5·343	6·729	9·505	11·393
		8	1·324	3·038	4·801	6·375	7·413	9·918
		10	1·323	3·034	4·722	6·300	7·082	9·348
		12	1·323	3·034	4·718	6·289	7·028	9·068
		13	1·323	3·034	4·717	6·287	7·024	9·038
		14	1·323	3·034	4·717	6·287	7·023	9·028
	0·2	6	1·209	2·612	4·070	5·066	6·571	7·666
		8	1·206	2·587	3·849	4·885	5·517	7·033
		10	1·206	2·586	3·821	4·858	5·368	6·803
		12	1·206	2·585	3·819	4·855	5·347	6·704
		13	1·206	2·585	3·819	4·855	5·346	6·694
		14	1·206	2·585	3·819	4·855	5·345	6·691
90	0·001	6	1·482	3·292	5·813	8·473	12·983	15·962
		8	1·465	3·040	5·349	5·559	9·022	9·814
		10	1·465	3·011	5·019	5·441	7·836	8·695
		12	1·464	3·009	4·990	5·436	7·567	8·587
		13	1·465	3·009	4·990	5·435	7·527	8·569
		14	1·465	3·009	4·989	5·435	7·523	8·561
	0·1	6	1·402	2·859	4·755	4·980	8·571	10·029
		8	1·398	2·792	4·502	4·814	6·957	7·410
		10	1·397	2·787	4·467	4·796	6·536	7·236
		12	1·397	2·787	4·464	4·794	6·490	7·208
		13	1·397	2·787	4·463	4·793	6·487	7·204
		14	1·397	2·787	4·463	4·793	6·486	7·204
	0·2	6	1·270	2·433	3·763	3·897	5·960	6·660
		8	1·268	2·395	3·642	3·810	5·255	5·497
		10	1·268	2·393	3·626	3·801	5·061	5·408
		12	1·268	2·392	3·625	3·800	5·041	5·394
		13	1·268	2·392	3·625	3·799	5·039	5·393
		14	1·268	2·392	3·625	3·799	5·039	5·393

(17). Standard eigenvalue problem solvers can be used to solve this equation. EISPACK [17] routines have been used in this study. The natural frequencies are given by the square roots of the eigenvalues. For convenience, a non-dimensional natural frequency parameter λ has been defined as

$$\lambda = (\Omega a^2/\pi^2)\sqrt{\rho t/D}. \tag{23}$$

3. NUMERICAL RESULTS AND DISCUSSION

In this section, numerical results of natural frequency parameter λ are presented for a range of triangular plate geometries and for different combinations of edge support conditions. In the numerical calculations, the shear correction factor κ has been assigned a conventionally used value of 5/6 and the Poisson ratio v has been assumed to be 0·3. Gauss quadrature with 20 points in each direction has been used in the numerical integration of stiffness and mass matrices of the plate. A three letter symbol consisting of

TABLE 2

Comparison of frequency parameters λ

Boundary conditions	b/a	$\alpha(^\circ)$	t/a	Source	Mode sequence number 1	2	3	4
CCC	1·0	90	0·001	Present	9·503	15·988	19·741	24·655
				[18]	9·510	15·978	19·737	24·601
	2·0		0·001	Present	5·415	8·355	11·518	12·357
				[18]	5·416	8·351	11·500	12·351
S*S*S*	1·0	90	0·001	Present	5·000	9·999	13·000	17·005
				[19]	5·000	10·000	13·000	17·002
	2·0		0·001	Present	2·813	5·054	7·569	8·241
				[19]	2·813	5·054	7·566	8·239
SCF	0·5	90	0·001	Present	9·214	18·156	26·491	29·184
				[20]	9·139	18·108	26·319	29·083
	2·0		0·001	Present	1·465	3·009	4·989	5·435
				[20]	1·450	2·984	4·955	5·408
CFC	1.0	90	0·001	Present	2·948	6·440	9·104	11·765
				[20]	2·925	6·380	9·083	11·662
	2·0		0·001	Present	1·563	3·089	4·944	5·675
				[20]	1·551	3·062	4·905	5·657
CFF	0·5	90	0·05	Present	2·179	5·773	10·621	11·164
				[12]	2·169	5·761	10·549	11·181
			0·20	Present	1·840	3·972	6·072	6·887
				[12]	1·840	4·001	6·091	–
		120	0·05	Present	2·060	5·862	10·307	12·216
				[12]	2·049	5·840	10·572	12·218
			0·20	Present	1·718	3·965	5·699	6·681
				[12]	1·718	3·985	5·652	6·734
		150	0·05	Present	2·311	8·685	13·841	20·315
				[12]	2·282	8·613	13·588	–
			0·20	Present	1·850	3·931	5·602	6·490
				[12]	1·837	3·904	5·607	–
	2·0	90	0·05	Present	0·167	0·715	1·216	1·739
				[12]	0·166	0·709	1·216	1·721
			0·20	Present	0·164	0·670	1·000	1·530
				[12]	0·163	0·666	1·001	–
		120	0·05	Present	0·155	0·648	1·312	1·690
				[12]	0·154	0·643	1·306	1·677
			0·20	Present	0·151	0·609	1·051	1·416
				[12]	0·150	0·605	1·051	–
		150	0·05	Present	0·161	0·688	1·616	2·411
				[12]	0·160	0·682	1·605	2·383
			0·20	Present	0·155	0·637	1·265	1·460
				[12]	0·154	0·632	1·266	–

TABLE 3

*Frequency parameters λ for CCC and S*S*S* plates*

			Mode sequence number					
b/a	$\alpha(^\circ)$	t/a	1	2	3	4	5	6
			(a) Boundary condition CCC					
0·5	45	0·001	31·373	48·310	64·222	75·160	87·409	103·649
		0·20	11·010	14·543	17·536	19·208	21·108	22·769
	90	0·001	21·661	33·433	46·383	49·678	63·510	69·432
		0·20	8·881	11·832	14·674	15·233	17·809	18·836
	135	0·001	48·861	66·741	86·696	117·335	128·847	156·869
		0·20	13·768	16·619	19·341	21·873	24·309	24·547
1·0	45	0·001	12·676	22·416	25·890	34·422	40·566	43·344
		0·20	6·419	9·494	10·450	12·749	14·110	14·829
	90	0·001	9·503	15·988	19·741	24·655	28·379	34·234
		0·20	5·302	7·657	8·882	10·349	11·362	12·883
	135	0·001	21·854	30·719	39·947	54·663	56·620	72·569
		0·20	8·747	10·850	12·703	14·673	15·879	16·799
2·0	45	0·001	7·844	12·067	16·026	18·765	21·979	25·674
		0·20	4·636	6·324	7·746	8·620	9·484	10·556
	90	0·001	5·415	8·355	11·518	12·357	15·754	17·162
		0·20	3·569	4·952	6·285	6·604	7·759	8·293
	135	0·001	12·228	16·550	22·205	27·880	32·259	38·997
		0·20	6·099	7·456	8·728	9·941	11·380	11·652
			(b) Boundary condition S*S*S*					
0·5	45	0·001	16·233	29·096	41·456	50·299	59·668	72·863
		0·20	8·878	13·076	16·273	16·416	16·416	16·416
	90	0·001	11·249	20·217	30·338	33·001	43·835	49·022
		0·20	6·847	10·346	13·495	14·301	16·416	16·416
	135	0·001	24·489	36·537	50·244	67·789	84·674	97·494
		0·20	11·634	14·926	16·416	16·416	16·416	16·460
1·0	45	0·001	6·715	14·265	17·049	24·029	29·298	31·618
		0·20	4·642	8·190	9·301	11·721	13·337	14·014
	90	0·001	5·000	9·999	13·000	17·005	20·059	25·064
		0·20	3·684	6·356	7·700	9·347	10·390	12·086
	135	0·001	11·065	17·189	23·425	32·906	37·271	45·480
		0·20	6·743	9·248	11·256	13·385	15·106	15·896
2·0	45	0·001	4·062	7·274	10·364	12·581	14·901	17·990
		0·20	3·118	5·002	6·526	7·565	8·479	9·619
	90	0·001	2·813	5·054	7·569	8·241	10·784	12·164
		0·20	2·291	3·754	5·180	5·552	6·768	7·402
	135	0·001	6·124	9·096	12·534	16·348	21·119	23·216
		0·20	4·318	5·891	7·288	8·618	10·171	10·833

a combination of letters, C, F, S and S* is used here to denote the support edge conditions of the triangular plate. The first, second and third letters represent, respectively, the support conditions along the edges AB, BC and CA (see Figure 1(a)). For instance, the symbol SCF is used to denote a plate simply-supported (first kind) along AB, clamped along BC and free along CA.

The convergence of λ with different polynomial degrees p_s for a number of representative triangular plate geometries and several combinations of boundary conditions was studied

first. Results of this study for an SCF plate with aspect ratio (b/a) of 2 and three values of relative thickness (t/a) are presented in Table 1. For all results presented in this paper, equal values have been assigned to p_1, p_2 and p_3 (i.e. $p_1 = p_2 = p_3$). Convergence of the frequency parameters of the first six modes of vibration corresponding to $\alpha = 45^\circ$ and 90° and 135° is reported in Table 1. It is observed that: the convergence pattern is monotonic; convergence is faster for thick plates than for thin plates; and lower modes converge faster

TABLE 4

*Frequency parameters λ for SCC and S*CC plates*

			Mode sequence number					
b/a	$\alpha(^\circ)$	t/a	1	2	3	4	5	6
			(a) Boundary condition SCC					
0·5	45	0·001	23·912	39·055	53·058	63·258	73·550	87·990
		0·20	10·065	13·949	17·129	18·874	20·275	20·859
	90	0·001	17·197	27·931	39·692	42·652	55·244	60·829
		0·20	8·128	11·335	14·350	15·007	17·499	18·714
	135	0·001	39·012	54·475	72·795	93·477	111·320	132·741
		0·20	12·933	16·067	18·809	21·280	21·932	23·461
1·0	45	0·001	10·261	19·236	22·439	30·384	36·240	38·804
		0·20	5·815	9·081	10·173	12·410	13·971	14·651
	90	0·001	7·993	14·067	17·601	22·195	25·695	31·312
		0·20	4·836	7·349	8·589	10·108	11·160	12·698
	135	0·001	18·450	26·547	34·581	47·445	50·521	61·661
		0·20	8·200	10·498	12·369	14·364	15·788	16·534
2·0	45	0·001	6·846	10·872	14·609	17·196	19·956	23·900
		0·20	4·284	6·079	7·506	8·431	9·285	10·421
	90	0·001	4·828	7·646	10·685	11·490	14·629	16·128
		0·20	3·312	4·753	6·102	6·416	7·611	8·152
	135	0·001	10·874	15·048	19·371	25·271	29·684	34·695
		0·20	5·762	7·228	8·506	9·738	11·225	11·504
			(b) Boundary condition S*CC					
0·5	45	0·001	23·911	39·053	53·057	63·258	73·553	87·994
		0·20	9·911	13·549	16·840	18·718	19·149	19·972
	90	0·001	17·197	27·931	39·691	42·651	55·258	60·834
		0·20	8·034	11·106	14·125	14·913	17·167	18·522
	135	0·001	39·007	54·472	72·811	93·478	111·312	132·819
		0·20	12·801	15·658	18·470	20·086	21·043	21·888
1·0	45	0·001	10·261	19·236	22·439	30·384	36·240	38·804
		0·20	5·744	8·925	10·125	12·237	13·838	14·594
	90	0·001	7·993	14·067	17·601	22·195	25·695	31·312
		0·20	4·787	7·289	8·487	10·079	11·041	12·569
	135	0·001	18·448	26·547	34·582	47·449	50·520	61·673
		0·20	8·141	10·380	12·223	14·198	15·701	16·368
2·0	45	0·001	6·846	10·872	14·609	17·196	19·957	23·902
		0·20	4·249	6·050	7·428	8·398	9·240	10·354
	90	0·001	4·828	7·646	10·686	11·490	14·628	16·128
		0·20	3·285	4·737	6·062	6·374	7·598	8·109
	135	0·001	10·874	15·048	19·372	25·274	29·684	34·697
		0·20	5·731	7·197	8·454	9·668	11·171	11·484

TABLE 5

*Frequency parameters λ for FS*S* and CS*S* plates*

			Mode sequence number					
b/a	$\alpha(^\circ)$	t/a	1	2	3	4	5	6
			(a) Boundary condition FS*S*					
0·5	45	0·001	2·433	8·249	15·214	22·577	26·683	34·972
		0·20	1·610	4·371	6·465	8·277	10·409	11·584
	90	0·001	2·554	7·167	13·642	16·826	22·224	28·081
		0·20	1·777	4·030	6·074	8·204	8·884	10·651
	135	0·001	4·589	11·140	18·774	27·351	36·507	46·720
		0·20	2·038	3·394	4·917	6·800	8·885	11·115
1·0	45	0·001	1·795	6·090	9·029	12·633	17·934	20·189
		0·20	1·453	4·118	5·713	7·039	9·173	9·938
	90	0·001	1·754	5·171	7·393	10·610	12·850	16·966
		0·20	1·430	3·682	4·908	6·345	7·529	8·985
	135	0·001	3·223	7·743	12·153	16·816	21·987	24·391
		0·20	1·947	3·918	5·579	7·206	8·467	10·237
2·0	45	0·001	1·762	4·354	6·406	8·763	10·173	12·956
		0·20	1·421	3·255	4·338	5·725	6·192	7·556
	90	0·001	1·409	3·403	5·073	5·907	8·338	9·345
		0·20	1·219	2·667	3·747	4·234	5·545	6·040
	135	0·001	2·551	5·553	7·791	10·438	14·002	14·802
		0·20	1·746	3·711	4·862	6·044	6·921	8·144
			(b) Boundary condition CS*S*					
0·5	45	0·001	22·305	36·960	50·886	60·651	71·157	85·377
		0·20	9·526	13·533	16·514	17·619	18·738	19·305
	90	0·001	14·743	24·823	35·912	38·860	51·077	56·238
		0·20	7·512	10·813	13·837	14·571	16·764	17·125
	135	0·001	31·254	45·303	61·440	79·827	97·536	114·606
		0·20	12·111	15·207	16·559	17·141	17·612	18·195
1·0	45	0·001	8·614	16·960	20·031	27·494	33·135	35·653
		0·20	5·234	8·651	9·666	12·055	13·640	14·187
	90	0·001	6·133	11·606	14·772	19·101	22·243	27·550
		0·20	4·152	6·710	8·087	9·586	10·674	12·369
	135	0·001	13·206	20·197	26·971	37·120	41·417	49·680
		0·20	7·264	9·590	11·535	13·569	15·333	16·069
2·0	45	0·001	4·763	8·234	11·480	13·799	16·187	19·605
		0·20	3·468	5·286	6·813	7·829	8·671	9·825
	90	0·001	3·226	5·615	8·252	8·935	11·485	13·016
		0·20	2·540	3·980	5·391	5·793	6·935	7·586
	135	0·001	6·878	10·207	13·633	18·079	22·520	25·451
		0·20	4·653	6·148	7·511	8·812	10·332	11·016

than the higher modes. It was found from the convergence study that a p_s value of more than 12 is necessary to generate reasonably accurate results for λ. In all subsequent computations, a value of 14 has been used to ensure accuracy.

Frequency parameters determined using the proposed method have been compared with those from the literature for specific triangular plate geometries and thicknesses as reported in Table 2. Results of Gorman [18, 19, 20] for CCC, S*S*S*, SCF and CFC plates are reported in this table. Since Gorman's frequency parameters are available only for thin

plates, his results are compared with the present results with a t/a value of 0·001. McGee and Butalia [12] have presented numerical results for natural frequencies for both thin and thick CFF triangular plates. Their results were based on a finite element method that was formulated using a higher order shear deformation theory. These results are compared with the present results for t/a equal to 0·5 and 0·20 in Table 2. The incorporation of the higher order shear deformation theory in [12] resulted in nine-degrees-of-freedom per node and this led to a dramatic increase in the problem size. It can be observed from Table 2 that

TABLE 6

Frequency parameters λ for FCC and CFF plates

			Mode sequence number					
b/a	$\alpha(^\circ)$	t/a	1	2	3	4	5	6
			(a) Boundary condition FCC					
0·5	45	0·001	8·430	16·806	25·830	33·178	38·991	50·323
		0·20	5·215	8·288	11·010	12·161	14·345	16·006
	90	0·001	7·097	13·826	22·255	23·893	33·250	37·205
		0·20	4·441	7·206	9·637	10·193	12·946	13·354
	135	0·001	14·753	24·663	36·438	51·112	62·699	71·083
		0·20	7·211	10·179	13·110	14·892	16·486	17·966
1·0	45	0·001	4·674	10·536	13·235	18·633	23·740	26·452
		0·20	3·270	6·009	6·841	9·039	10·315	11·301
	90	0·001	4·166	8·784	11·046	15·393	17·783	22·155
		0·20	2·939	5·221	6·026	7·865	8·665	9·848
	135	0·001	8·404	15·113	21·887	28·123	32·257	41·369
		0·20	4·789	7·377	9·254	10·812	11·504	13·260
2·0	45	0·001	3·964	7·538	10·005	12·511	14·963	18·186
		0·20	2·790	4·608	5·654	6·645	7·672	8·631
	90	0·001	3·124	5·622	7·954	8·664	11·762	12·926
		0·20	2·328	3·688	4·873	5·174	6·497	6·909
	135	0·001	5·941	10·574	13·724	18·258	21·252	24·311
		0·20	3·659	5·737	6·795	7·953	8·869	9·425
			(b) Boundary condition CFF					
0·5	45	0·001	4·819	11·403	18·737	24·540	31·726	38·466
		0·20	3·486	6·403	8·938	10·700	12·695	14·510
	90	0·001	2·230	6·104	11·517	12·158	19·459	24·254
		0·20	1·840	3·972	6·072	6·887	9·559	10·512
	135	0·001	2·229	7·393	12·533	17·277	21·902	27·535
		0·20	1·758	4·304	5·464	7·086	8·464	9·933
1·0	45	0·001	1·310	4·422	5·892	10·312	14·124	14·707
		0·20	1·157	3·118	3·968	6·204	7·568	7·844
	90	0·001	0·625	2·377	3·310	5·689	7·743	10·063
		0·20	0·582	1·900	2·408	3·936	4·980	5·847
	135	0·001	0·593	2·335	4·222	6·487	7·609	11·251
		0·20	0·540	1·885	2·489	3·674	4·630	5·135
2·0	45	0·001	0·280	1·154	1·919	2·892	4·185	5·756
		0·20	0·271	1·029	1·444	2·276	3·001	3·762
	90	0·001	0·168	0·720	1·252	1·764	2·958	3·368
		0·20	0·164	0·670	1·000	1·530	2·194	2·632
	135	0·001	0·157	0·664	1·487	2·003	2·869	3·868
		0·20	0·151	0·616	1·151	1·434	2·145	2·515

TABLE 7

*Frequency parameters λ for SCF and S*CF plates*

			Mode sequence number					
b/a	$\alpha(^\circ)$	t/a	1	2	3	4	5	6
			(a) Boundary condition SCF					
0·5	45	0·001	9·158	21·850	30·134	40·737	47·192	59·562
		0·20	5·096	10·016	12·109	14·714	15·594	17·631
	90	0·001	9·214	18·156	26·491	29·184	40·375	44·972
		0·20	5·452	8·695	11·492	12·004	14·844	15·963
	135	0·001	21·117	34·397	45·817	59·154	75·808	77·212
		0·20	9·008	12·749	15·243	16·888	18·805	20·584
1·0	45	0·001	2·770	7·672	10·829	14·772	20·497	22·802
		0·20	2·181	5·001	6·452	8·029	10·141	10·919
	90	0·001	3·220	7·376	9·559	13·486	15·776	20·031
		0·20	2·488	4·838	5·752	7·550	8·390	9·680
	135	0·001	7·718	13·346	18·408	24·637	29·077	33·420
		0·20	4·644	7·132	8·833	10·713	11·170	12·910
2·0	45	0·001	1·381	3·301	5·290	7·290	8·289	10·941
		0·20	1·206	2·585	3·819	4·855	5·345	6·691
	90	0·001	1·465	3·009	4·989	5·435	7·523	8·561
		0·20	1·268	2·392	3·625	3·799	5·039	5·393
	135	0·001	3·479	5·725	8·194	10·810	13·778	15·574
		0·20	2·558	3·856	5·139	6·190	7·086	7·724
			(b) Boundary condition S*CF					
0·5	45	0·001	9·158	21·849	30·133	40·736	47·190	59·565
		0·20	4·668	8·694	11·149	13·655	14·560	16·717
	90	0·001	9·214	18·156	26·490	29·184	40·376	44·973
		0·20	5·285	8·400	11·236	11·746	14·567	15·331
	135	0·001	21·116	34·397	45·814	59·160	75·806	77·208
		0·20	8·805	12·552	14·966	16·715	18·185	19·173
1·0	45	0·001	2·770	7·671	10·829	14·772	20·496	22·802
		0·20	2·086	4·684	6·393	7·399	9·862	10·168
	90	0·001	3·220	7·376	9·559	13·486	15·776	20·030
		0·20	2·428	4·812	5·561	7·523	8·312	9·383
	135	0·001	7·718	13·346	18·408	24·638	29·078	33·422
		0·20	4·555	7·104	8·689	10·594	11·119	12·770
2·0	45	0·001	1·381	3·301	5·290	7·290	8·289	10·942
		0·20	1·169	2·533	3·693	4·822	5·186	6·479
	90	0·001	1·465	3·009	4·989	5·435	7·523	8·561
		0·20	1·244	2·380	3·598	3·728	5·033	5·330
	135	0·001	3·479	5·725	8·194	10·810	13·778	15·574
		0·20	2·558	3·856	5·139	6·190	7·086	7·724

the present results are generally in good agreement with those from the literature. The agreement is very good for thick plates.

Frequency parameters computed for different combinations of boundary conditions in a thin plate (with $t/a = 0{\cdot}001$) and a thick-plate (with $t/a = 0{\cdot}2$) are presented in Tables 3–7. These tables are for b/a equal to 0·5, 1·0 and 2·0, and for each b/a value three values of α (45°, 90° and 135°) have been considered. Results are presented for CCC, S*S*S*, SCC, S*CC, FS*S*, CS*S*, FCC, CFF, SCF and S*CF plates. It is seen from

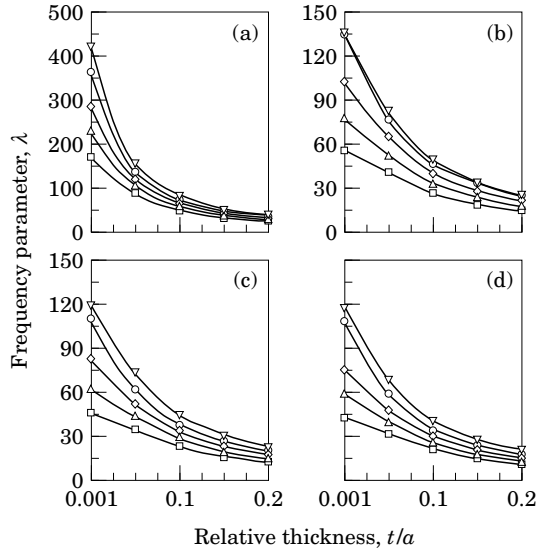

Figure 2. Variation of frequency parameter, λ, with relative thickness, t/a, and aspect ratio, b/a for CCC plate when $\alpha = 15^\circ$. Mode numbers: –□–, 1; –△–, 2; –◇–, 3; –○–, 4; –▽–, 5. b/a: (a) 0·5, (b) 1·0; (c) 1·5; (d) 2·0.

these tables that changing the boundary conditions from clamped to simply-supported and from simply-supported to free leads to a reduction in λ due to the reduced constraint at the boundaries. It is evident from Tables 4 and 7 that there is almost no difference in the frequencies calculated for S and S* boundary conditions in thin plates. For thick plates, however, it appears that the S edge condition leads to slightly higher frequencies than the S* edge condition. This can be explained by recalling that the S condition requires the transverse deflection and tangential rotation to be zero while the S* condition requires only the transverse deflection along the support to be zero. Therefore, the added constraint in

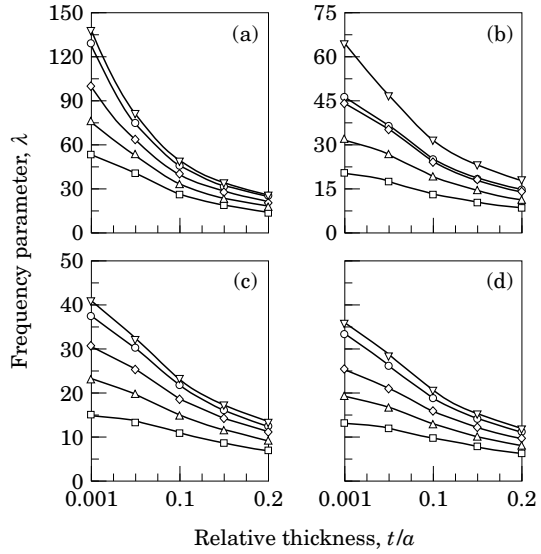

Figure 3. Variation of frequency parameter, λ, with relative thickness, t/a, and aspect ratio, b/a, for CCC plate when $\alpha = 30^\circ$. Mode number symbols and b/a values as for Figure 2.

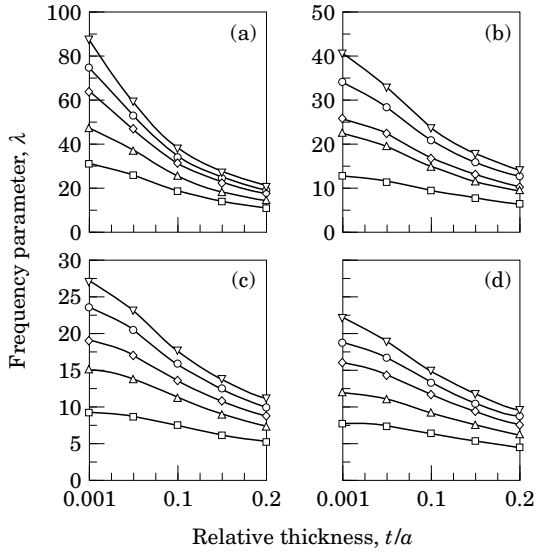

Figure 4. Variation of frequency parameter, λ, with relative thickness, t/a, and aspect ratio, b/a, for CCC plate when $\alpha = 45^\circ$. Mode number symbols and b/a values as for Figure 2.

the S condition causes a slight increase in λ values. It can be observed that these increases are significant for lower b/a values. As seen from the last rows of the (a) and (b) parts of Tables 4 and 7, the increase in λ is slight or negligible for higher values of b/a.

It is believed that the frequency parameters in Tables 3–7 will be useful to design engineers for checking natural frequency calculations and may also serve as benchmark values for those who are developing numerical techniques and software packages for determining vibration frequencies of thick triangular plates.

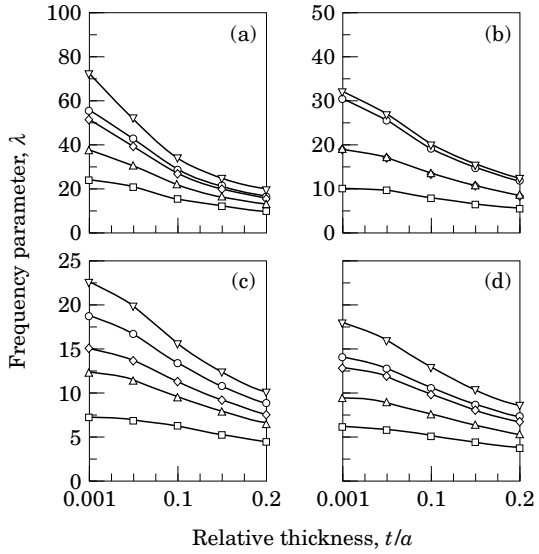

Figure 5. Variation of frequency parameter, λ, with relative thickness, t/a, and aspect ratio, b/a, for CCC plate when $\alpha = 60^\circ$. Mode number symbols and b/a values as for Figure 2.

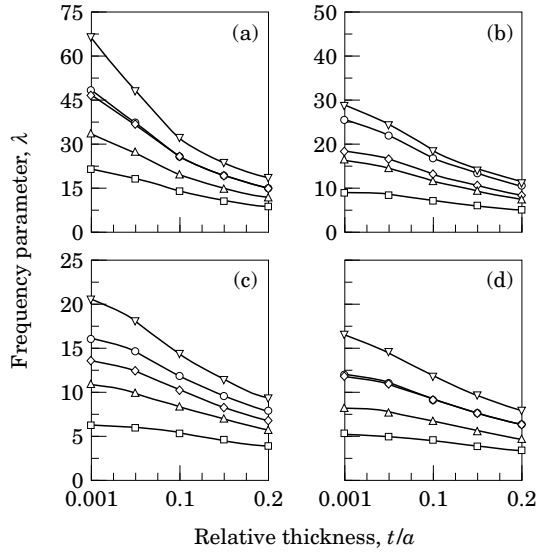

Figure 6. Variation of frequency parameter, λ, with relative thickness, t/a, and aspect ratio, b/a, for CCC plate when $\alpha = 75^\circ$. Mode number symbols and b/a values as for Figure 2.

A comprehensive set of natural frequency parameters corresponding to the lowest five modes of vibration in CCC plates are presented in Figures 2–12. These figures depict the variation of λ with relative plate thickness (t/a), aspect ratio (b/a) and internal angle α. Results are presented for four values of b/a (0·5, 1·0, 1·5 and 2·0) while α has been varied from 15° to 165° in steps of 15°. The relative thickness has been varied from a very thin plate value (0·001) to a thick plate value (0·2). The figures show that, for given b/a and α, frequencies decrease as relative thickness increases. This clearly demonstrates the influence of shear deformation and rotary inertia on natural frequencies—as thicker plates

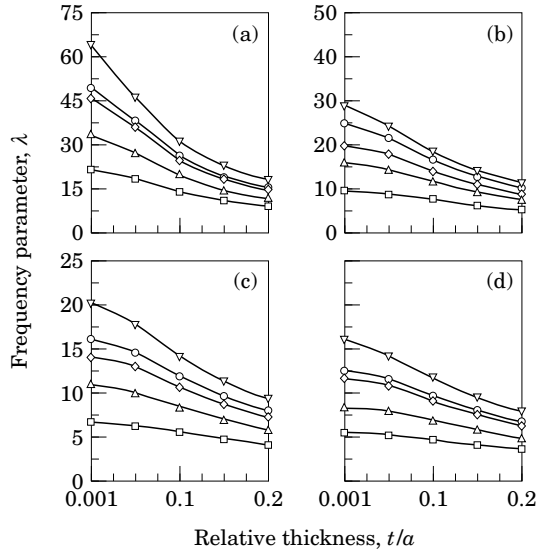

Figure 7. Variation of frequency parameter, λ, with relative thickness, t/a, and aspect ratio, b/a, for CCC plate when $\alpha = 90^\circ$. Mode number symbols and b/a values as for Figure 2.

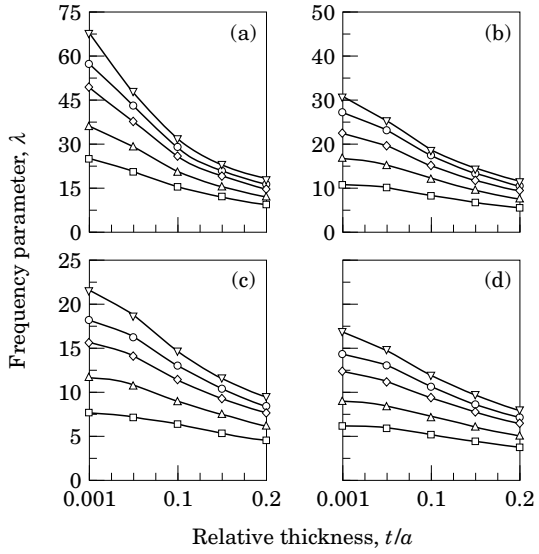

Figure 8. Variation of frequency parameter, λ, with relative thickness, t/a, and aspect ratio, b/a, for CCC plate when $\alpha = 105^\circ$. Mode number symbols and b/a values as for Figure 2.

have greater shear deformation and rotary inertia contribution. It can be observed from the figures that, for the same α, frequencies for each mode decrease with increasing values of b/a. Furthermore, for the same b/a, a gradual decrease of λ with α can be seen as α increases to 90°. Thereafter, a gradual increase in λ is seen as α increases from 90° to 165°.

Finally, to see if node number ordering causes discrepancies in computed frequencies, a few checks have been made. For instance, for a CCC plate with $b/a = 1$, $\alpha = 45^\circ$ and

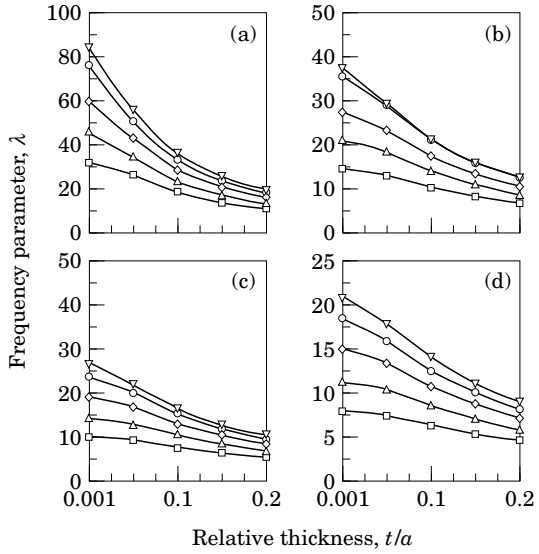

Figure 9. Variation of frequency parameter, λ, with relative thickness, t/a, and aspect ratio, b/a, for CCC plate when $\alpha = 120^\circ$. Mode number symbols and b/a values as for Figure 2.

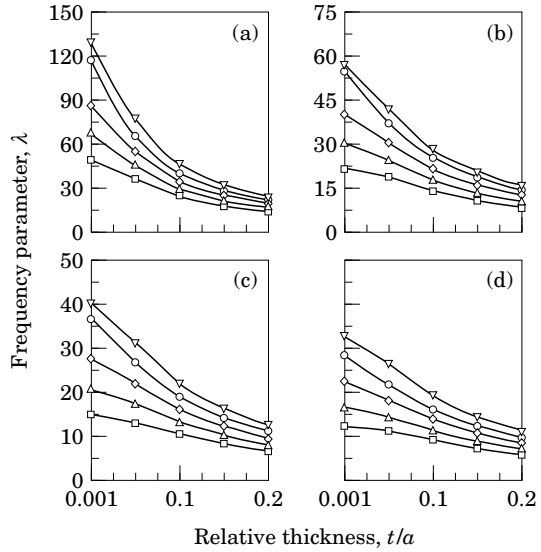

Figure 10. Variation of frequency parameter, λ, with relative thickness, t/a, and aspect ratio, b/a, for CCC plate when $\alpha = 135^\circ$. Mode number symbols and b/a values as for Figure 2.

$t/a = 0{\cdot}2$ (refer to Table 3), changing node number ordering from 1-2-3 to 2-3-1 (i.e. 1 to 2, 2 to 3 and 3 to 1) resulted in no change in the first six frequencies up to three decimal places. For the same plate with $b/a = 2$, changing node number ordering in the same way resulted in the fifth frequency increasing by 0·02% and the sixth frequency increasing by 0·08%. The first four frequencies remained unchanged up to three decimal places. Thus it seems that the discrepancy is very small. However, to avoid this discrepancy, the authors will consider using area co-ordinates in their future work in this area.

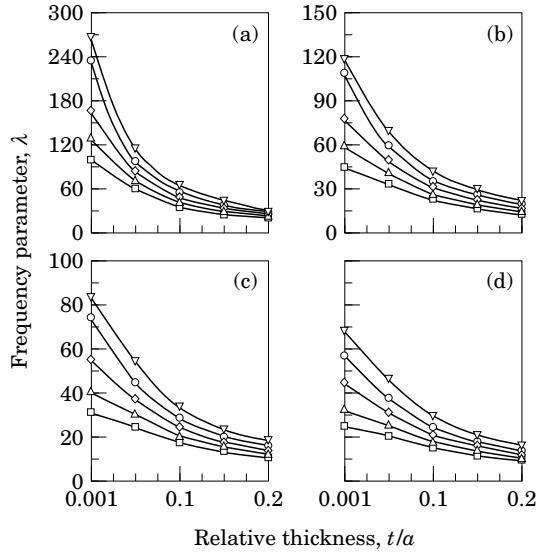

Figure 11. Variation of frequency parameter, λ, with relative thickness, t/a, and aspect ratio, b/a, for CCC plate when $\alpha = 150^\circ$. Mode number symbols and b/a values as for Figure 2.

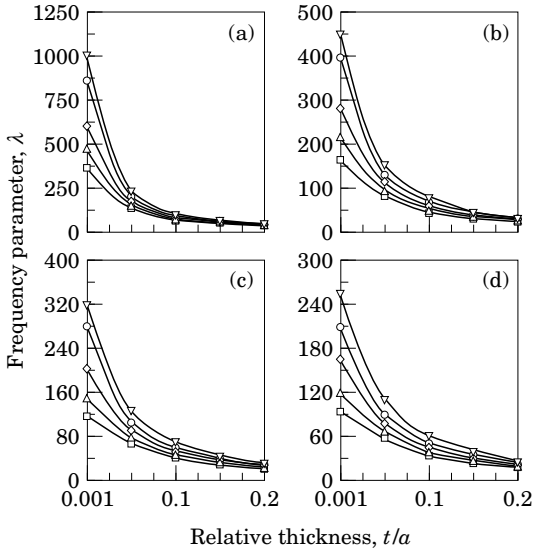

Figure 12. Variation of frequency parameter, λ, with relative thickness, t/a, and aspect ratio, b/a, for CCC plate when $\alpha = 165^\circ$. Mode number symbols and b/a values as for Figure 2.

4. CONCLUSIONS

The free vibration of shear deformable general triangular plates with arbitrary combinations of edge support conditions has been studied in this article. Effects of shear deformation and rotary inertia have been taken into account in the analysis by making use of the first order shear deformation theory of Reissner and Mindlin. The governing eigenvalue problem to solve for the natural frequencies has been formulated using the pb-2 Rayleigh–Ritz method.

Convergence of the natural frequencies has been investigated, and the accuracy of the computed natural frequencies has been established by comparing results with those from the literature for specific triangular plate geometries and thicknesses. Natural frequencies of a large number of triangular plates with different combination of free, simply supported and clamped support edge conditions have been tabulated. These tabulated results will be useful to design engineers for checking natural frequency calculations and may also serve as benchmark values for those who are developing numerical techniques and software packages for determining vibration frequencies of thick triangular plates.

A comprehensive parametric study of natural frequencies of general triangular plates with all three edges clamped has also been reported. No previous results are known to exist for general triangular shaped Mindlin plates having arbitrary combination to support edge conditions. The Rayleigh–Ritz method used for analysis has the advantage that it does not require any mesh descretization and, consequently, it needs only a very minimal amount of input data for computations.

REFERENCES

1. A. W. Leissa 1969 *Vibration of Plates* (NASA SP-160). Washington, D.C.: Office of Technology Utilization, NASA.
2. A. W. Leissa 1977 *The Shock and Vibration Digest* **9**, 13–24. Recent research in plate vibrations: classical theory.
3. A. W. Leissa 1981 *The Shock and Vibration Digest* **13**, 11–12. Plate vibration research 1976–1980: classical theory.

4. A. W. Leissa 1987 *The Shock and Vibration Digest* **19**, 11–18. Recent research in plate vibrations 1981–1985. Part I. classical theory.
5. C. S. Kim and S. M. Dickinson 1990 *Journal of Sound and Vibration* **141**, 291–312. The free flexural vibration of right triangular isotropic and orthotropic plates.
6. C. S. Kim and S. M. Dickinson 1992 *Journal of Sound and Vibration* **152**, 383–403. The free flexural vibration of isotropic and orthotropic general triangular shaped plates.
7. K. Y. Lam, K. M. Liew and S. T. Chow 1990 *International Journal of Mechanical Sciences* **32**, 455–464. Free vibration analysis of isotropic and orthotropic triangular plates.
8. B. Singh and S. Chakraverty 1992 *International Journal of Mechanical Sciences* **34**, 947–955. Transverse vibration of triangular plates using characteristic orthogonal polynomials in two variables.
9. O. G. McGee, A. W. Leissa and C. S. Huang 1992 *International Journal of Mechanical Sciences* **34**, 63–84. Vibrations of cantilevered skewed trapezoidal and triangular plates with corner stress singularities.
10. E. Reissner 1945 *American Society of Mechanical Engineers Journal of Applied Mechanics* **12**, 69–76. The effect of transverse shear deformation on the bending of elastic plates.
11. R. D. Mindlin 1951 *American Society of Mechanical Engineers Journal of Applied Mechanics* **18**, 1031–1036. Influence of rotary inertia and shear in flexural motion of isotropic elastic plates.
12. O. G. McGee and T. S. Butalia 1992 *Computers and Structures* **45**, 1033–1059. Natural vibrations of shear deformable cantilevered skewed trapezoidal and triangular thick plates.
13. S. Kitipornchai, K. M. Liew, Y. Xiang and C. M. Wang 1993 *International Journal of Mechanical Sciences* **35**, 89–102. Free vibration of isosceles triangular Mindlin plates.
14. K. M. Liew, Y. Xiang and S. Kitipornchai 1993 *Computers and Structures* **49**, 1–78. Transverse vibration of thick rectangular plates.
15. K. M. Liew, Y. Xiang, S. Kitipornchai and C. M. Wang 1993 *Journal of Sound and Vibration* **168**, 39–69. Vibration of thick skew plates based on Mindlin shear deformation plate theory.
16. Y. Xiang, K. M. Liew and S. Kitipornchai 1993 *American Society of Civil Engineers Journal of Engineering Mechanics* **119**, 1579–1599. Transverse vibration of thick annular sector plates.
17. B. J. Garbow, J. M. Boyle, J. J. Dongarra and C. B. Moler 1977 *Matrix eigensystem routines—EISPACK guide extension*. New York: Springer-Verlag.
18. D. J. Gorman 1986 *Journal of Sound and Vibration* **106**, 419–431. Free vibration analysis of right triangular plates with combinations of clamped-simply supported boundary conditions.
19. D. J. Gorman 1983 *Journal of Sound and Vibration* **89**, 107–118. A highly accurate analytical solution for free vibration analysis of simply supported right triangular plates.
20. D. J. Gorman 1989 *Journal of Sound and Vibration* **131**, 115–125. Accurate free vibration analysis of right triangular plates with one free edge.